Supplementary Information (SI) for Materials Advances.

Modified Pd-HPMo@GNP as an Efficient Electro/Nanocatalyst for Hydrogen Evolution Reaction and reduction of 4-Nitrophenol

Selvaraj Iniyan[b], Aathilingam Vijayaprabhakaran[a,b], Christy Sebastian,[b] Murugavel Kathiresan[a,b]*

[a] Academy of Scientific and Innovative Research (AcSIR), Ghaziabad- 201002, India.

[b] Electro organic and Materials Electrochemistry Division, CSIR-CECRI, Karaikudi, 630003, Tamil Nadu, India, Email: kathiresan@cecri.res.in

1. Materials and Methods

1. 1 Materials and Methods

Graphene nanopowder, phosphomolybdic acid, and palladium chloride were purchased from Sisco Research Laboratories Pvt. Ltd. Ethanol, Nafion solution (5 Wt%) were purchased from Sigma Aldrich. All the chemicals were used without further purification, and deionized water was used throughout the synthesis procedures.

An X-ray diffractometer (XRD, D8 Focus, Bruker, Germany) was used to analyze the morphology, phase structure, and crystalline nature of the synthesized materials using the source of the monochromated Cu Kα radiation (λ = 1.5418 Å). Every XRD pattern was captured at a scan rate of 5^{o} min^{-1} spanning the 2θ range of 5 – 80^{o}. Examining the chemical bonding and functionalities was done through Raman spectroscopy employing Lab RAM HR FT-Raman module with 532 nM LASER, The morphological traits, along with the elemental composition, were identified using Scanning Electron Microscopy (SEM) (Ultra 55 model, Zeiss Gemini) coupled with Energy-Dispersive X-ray spectroscopy (EDS). High Resolution-Transmission Electron Microscopy (HR-TEM) was taken using (Tecnai^{TM} G^2 TF20), at 200 kV and High Angle Angular Dark Field (HAADF) elemental mapping with Talos F-200-S. All the XPS data was collected from a Mg/Al X-ray photoelectron spectrometer (XPS) using a twin anode source and 300/400 W Theta Probe (MULTILAB 2000, Thermo Scientific, USA). The determination of the elemental composition of Pd and Mo in the Pd-HPMo@GNP sample was carried out using inductively coupled plasma mass spectrometer (ICP-MS), Agilent 7850 ICP-MS fitted with standard sample introduction kit & SPS4 Autosampler, analysis was performed using Helium collision gas technology to estimate the % composition quantity of Pd and Mo.

1.2 Preparation of Pd-HPMo:

Under the protection of an Ar atmosphere, 0.1108 g of $PdCl_2$ and 0.125 g of HPMo were mixed with steady stirring in 15 mL of ethanol solvent for 2 hours. After completion of this process, the product was washed with water and rinsed twice with ethanol to remove the surfactant and unreacted compounds. Finally, the precipitate was vacuum-dried in a rotary evaporator for 1 hour at 45° C and 175 mbar pressure.

1.3 Preparation of Pd-HPMo@GNP:

A small amount of 0.02 g of Pd-HPMo powder was dissolved in 12 mL of ethanol solvent, and magnetically stirring for about 10 minutes, a dispersed solution was formed. The resulting

solution was delivered dropwise into an Ar environment and mixed with 0.2 g Graphene Nanopowder packed in a 20 mL vessel. Following vigorous stirring and 2 hrs sonication, the products were obtained by filtering them using Whatman filter paper and drying them at room temperature, and they were abbreviated as Pd-HPMo@GNP (the mass of Pd-HPMo accounts for 10% of that of GNP).

1.4 Working Electrode fabrication: The electrodes for the electrochemical HER were prepared by the conventional drop casting method on carbon cloth (CC). The catalytic ink was prepared using water, ethanol, and Nafion solution (5 wt%) in the ratio of (7.5:2:0.5) to make 1 mL of the solution. 3 mg catalyst powder was added to it and sonicated for 15 minutes. Then 34.5 μL of the suspended solution was drop cast over the Carbon Cloth (0.5 cm^2) and dried at 60 ^{0}C (loading ~ 0.1035 mg cm^{-2}). Then, the dried electrode was used as a working electrode for the electrocatalytic studies throughout the experiment. For handling the chemicals and glassware for the synthesis process and the application part, safety gloves, lab coats, and safety glass were mandatory and used accordingly.

1.5 Electrochemical Characterizations:

The pristine HPMo, Pd-HPMo, and Pd-HPMo@GNP were applied for the water reduction study using 0.5 M H_2SO_4 solution. The electrochemical properties were measured using a Metrohm AUTOLAB instrument with CV, LSV, and chronoamperometry techniques. All the electrochemical experiments were carried out by employing a conventional three-electrode set-up. For the HER experiment, we used Carbon cloth (CC) as a working electrode, an Ag/AgCl (3 M KCl) electrode as a reference electrode, and a Graphite rod as a Counter electrode. The polarization studies were carried out at a slow scan rate of 2 mV s^{-1}. 85% iR compensation was done manually from the R_S value calculated from the EIS. Continuous rapid sweeping through accelerated degradation (AD) studies at a very high sweep rate of 100 mV s^{-1} for 1000 cycles were carried out in 0.5 M H_2SO_4. The Electrochemical Impedance Studies (EIS) were conducted in the frequency range of 0.1 Hz to 100 kHz. ECSA was determined using cyclic voltammetry (CV) measurements. The potential range within a non-Faradaic current response was determined from CV. In this work, the potential typically ranges from 0.125 V to 0.227 V (vs. RHE). CV measurements were conducted in quiescent solution by sweeping the potential across the non-Faradaic region at five different scan rates: 30, 60, 90, 120, and 150 mV s^{-1}.

$$E_{RHE} = E_{Ag/AgCl} + 0.210 + 0.059*pH \quad \text{……equation S1}$$

$$E_{iR\ compensated} = E_{measured} - R_s i_{measured} \quad \text{……equation S2}$$

All the potential data were converted into an RHE scale according to the following equation:

Overpotential

The overpotential values of all the catalysts were calculated at a benchmarking current density of 10 mA cm^{-2} by employing the following relation:

$$\eta_{10}(HER) = (0\text{-}E_{obs})\ V \text{ vs. RHE} \quad \text{equation S3}$$

The Tafel Slope

The Tafel slope was calculated by fitting the overpotential versus log (j) using the Tafel equation as given below:

$$\eta = b \times \log(j/j_o) \quad \text{equation S4}$$

Where "b" signifies the Tafel slope value, "j" implies the current density value, and "j_o" is the exchange current density.

Electrochemical Active Surface Area (ECSA) and Roughness Factor (R_f)

The double-layer capacitance (C_{dl}) was calculated as the slope of the linear relationship between the current density and scan rate. The C_{dl} was assessed through cyclic voltammetry (CV) at different scan speeds (v = 150, 120, 90, 60, 30 $mV \cdot s^{-1}$) by employing the following reaction:

$$C_{dl} = \Delta j/2v = |j_a - j_b|/2v \quad \text{equation S5}$$

Where (j_b is discharge current density and j_a is charge current density) and v is the scan rate.

Then, the Roughness factor (R_f) was achieved via the equation

$$R_f = C_{dl}/C_s \quad \text{equation S6}$$

Cs is the sample's specific capacitance or the capacitance of an atomically smooth planar surface of the material per unit area under identical electrolyte conditions. We use general specific capacitances of $Cs = 0.035$ mF cm^{-2} in 0.5 M H_2SO_4 based on typical reported values for our surface area estimates.

To calculate ECSA (ECSA = $R_f \times S$, S is the geometric area of the electrode). ECSA was obtained from the equation

$$ECSA = R_f \times S \quad \text{equation S7}$$

Where S is the geometric area of the working electrode.

Turnover Frequency (TOF):

The turnover frequency (TOF) of all the catalysts was calculated by using the following relation:

$$TOF = (j \times S) / (n \times F) \quad \text{.....equation S8}$$

Where "j" stands for the measured current density value at a particular overpotential value, "S" is the geometrical surface area of the working electrode (0.5 cm^2), and "n" stands for the number of electron transfers (For HER, n = 2), "F" is the Faraday constant with a numerical value of 96485 C mol^{-1}.

1.6 Catalytic reduction of *p*-nitrophenol:

A quartz cuvette with a path length of 1 cm was used to optimize the reduction process. This reaction was carried out to evaluate the catalytic performance of both Pd-HPMo and Pd-HPMo@GNP catalysts. 3 milligrams of 4-NP was dissolved in 50 mL of deionized water and sonicated for half an hour; the solution was light yellow. Then, $NaBH_4$ (120 mg) was added to the 4-NP solution. However, in the presence of Pd-HPMo@GNP (1 mg) catalysts, plenty of bubbles were detected, and the rate of gas release increased significantly. After completion of the reaction, the solution becomes colorless. UV-visible spectroscopy was employed to monitor the conversion of *p*-nitrophenol (PNP) to *p*-aminophenol (PAP) at room temperature.

2. Characterisation

2.1 Raman spectroscopy

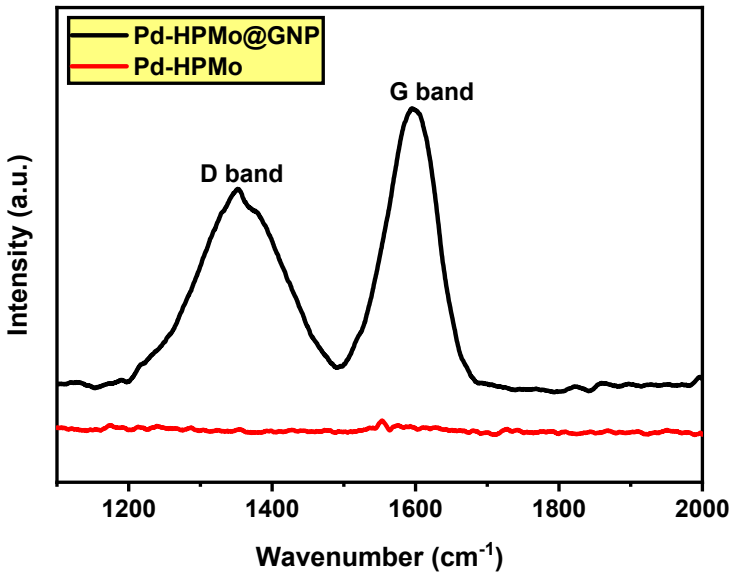

Figure S1 Raman spectrum of Pd-HPMo and Pd-HPMo@GNP.

2.2 Field emission scanning electron microscopy (FESEM) and Energy Dispersive X-ray spectroscopy (EDS)

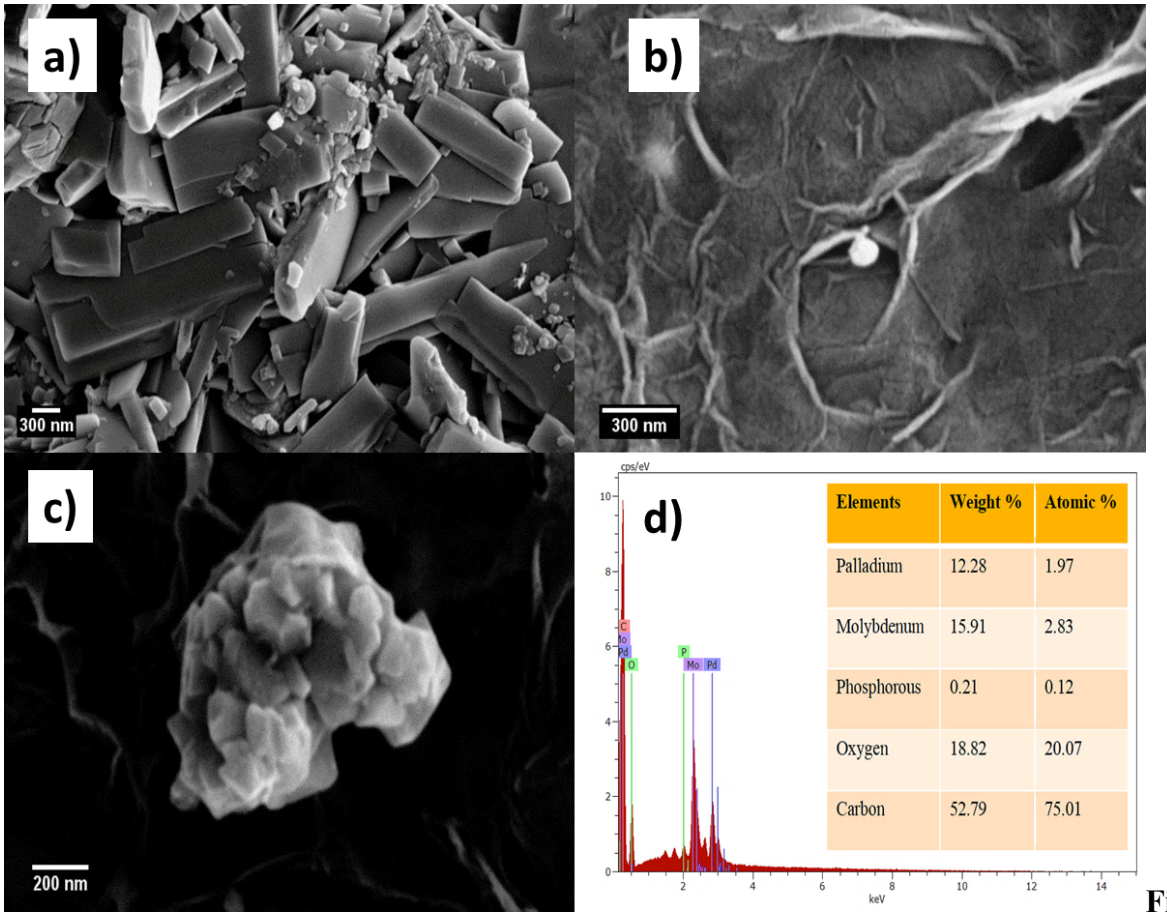

Elements	Weight %	Atomic %
Palladium	12.28	1.97
Molybdenum	15.91	2.83
Phosphorous	0.21	0.12
Oxygen	18.82	20.07
Carbon	52.79	75.01

Figure S2 (a) FESEM image of Pd-HPMo (b and c) Pd-HPMo@GNP at different Magnifications (d) EDAX data of PdHPMo@GNP.

2.3 HRTEM Analysis

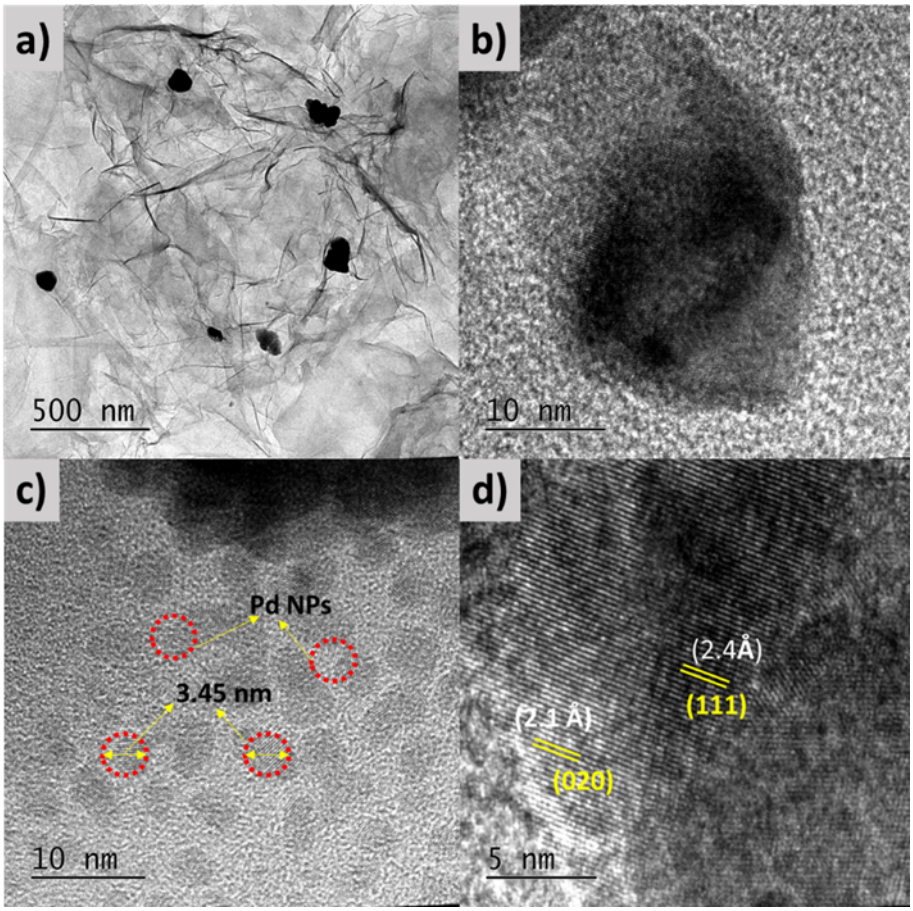

Figure S3. HRTEM image of an as-deposited Pd-HPMo nanoparticle.

Crossed lattice fringes from the 111 and 020 planes of Pd visible of Pd-HPMo@GNP.

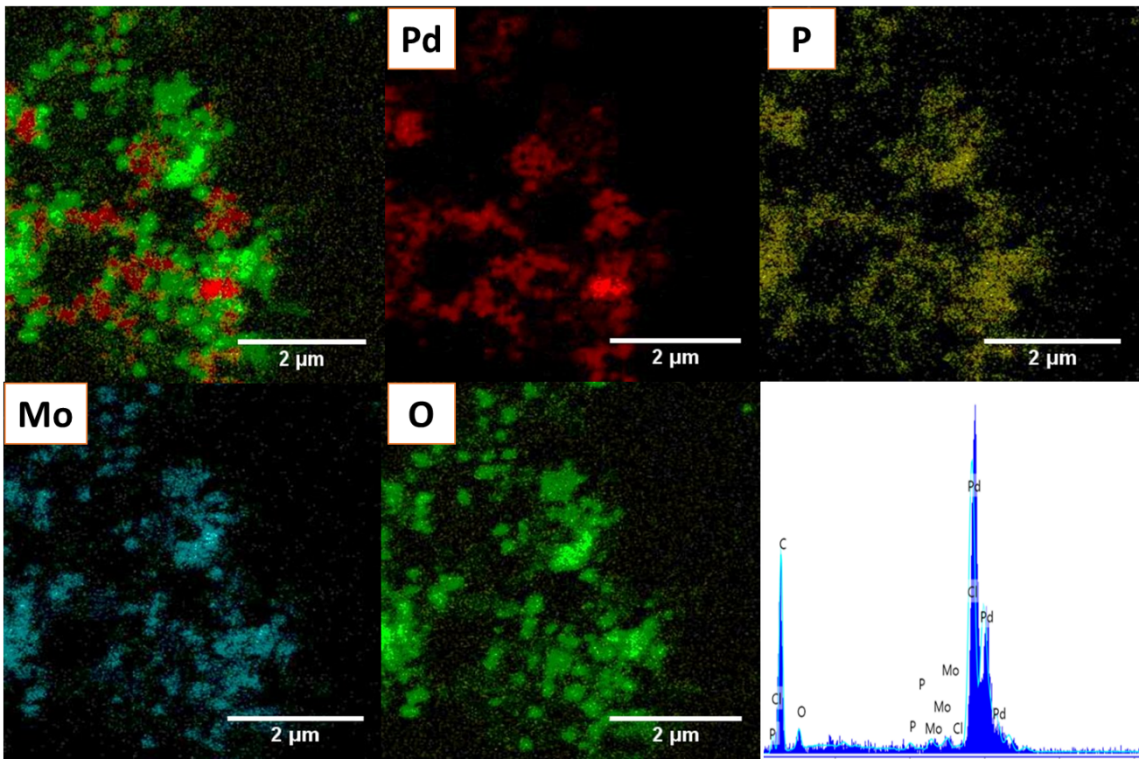

Figure S4. HRTEM elemental mapping of Pd-HPMo and EDAX of Pd-HPMo.

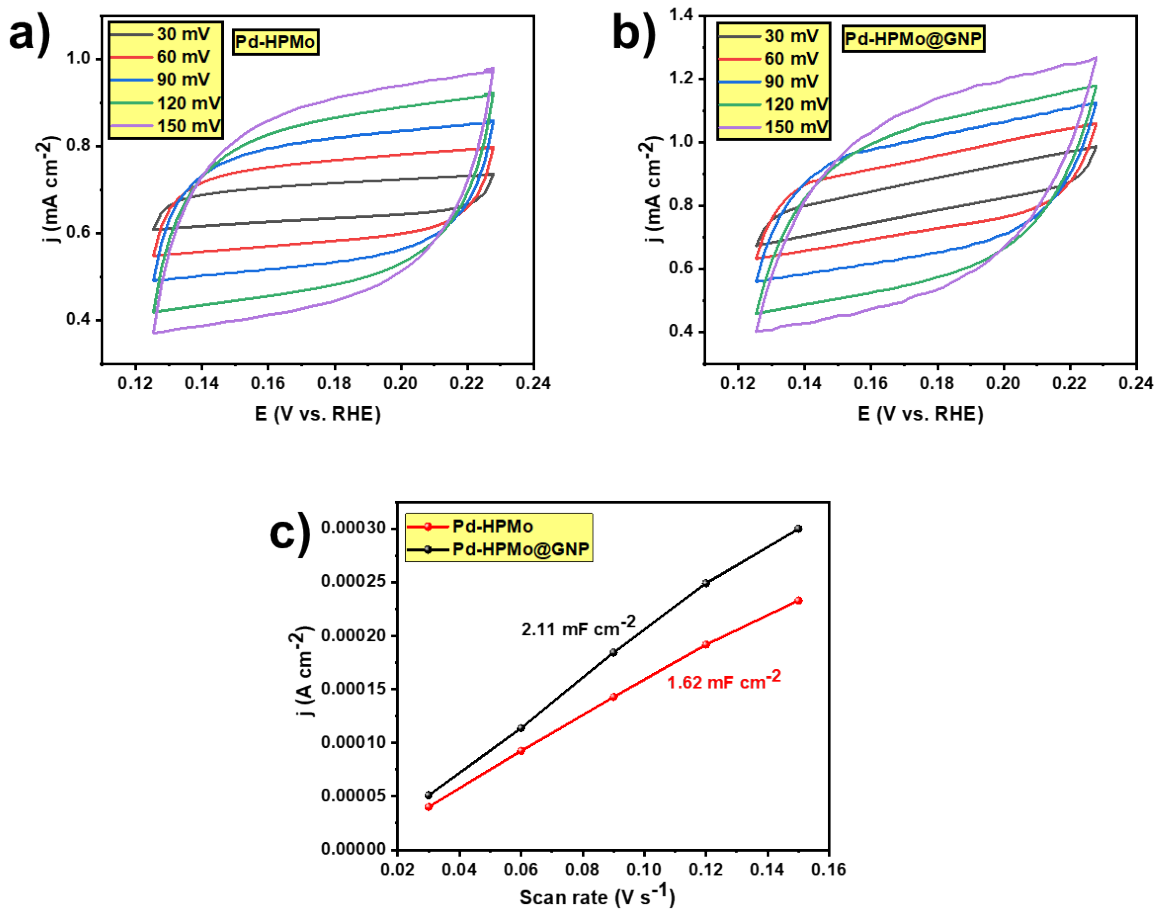

Figure S5. (a and b) are CVs measured at non-faradaic regions at different scan rates to measure the C_{dl} values of Pd-HPMo, Pd-HPMo@GNP respectively; (c) Corresponding calculated C_{dl} values of Pd-HPMo, Pd-HPMo@GNP.

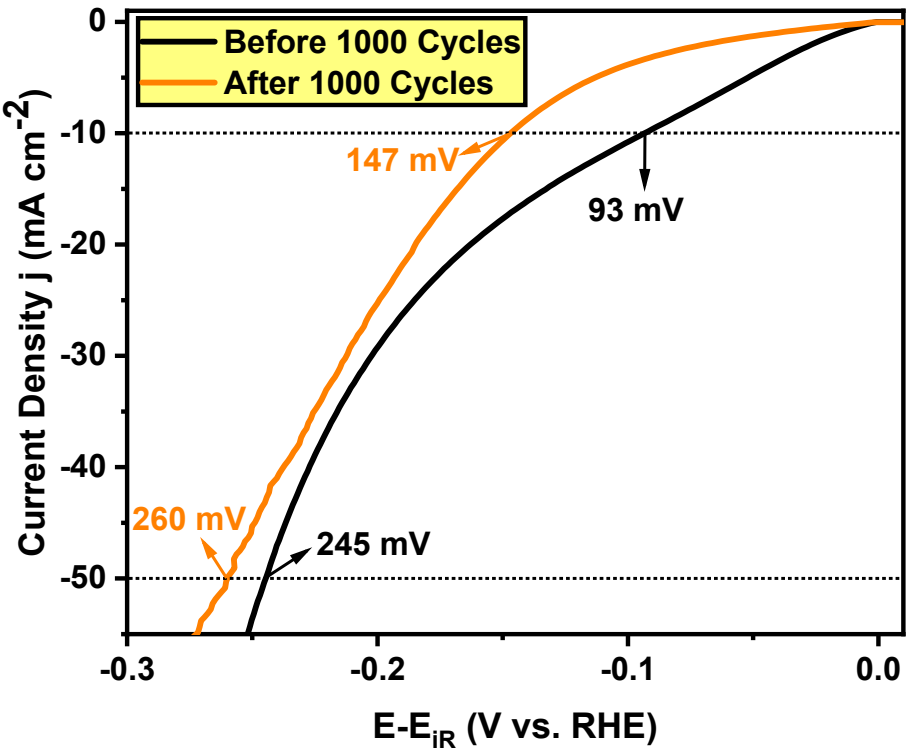

Figure S6. Acceleration degradation (AD) study for HER: The LSV results for the Pd-HPMo@GNP before and after 1000 CV cycles at scan rate 100 mV sec^{-1}.

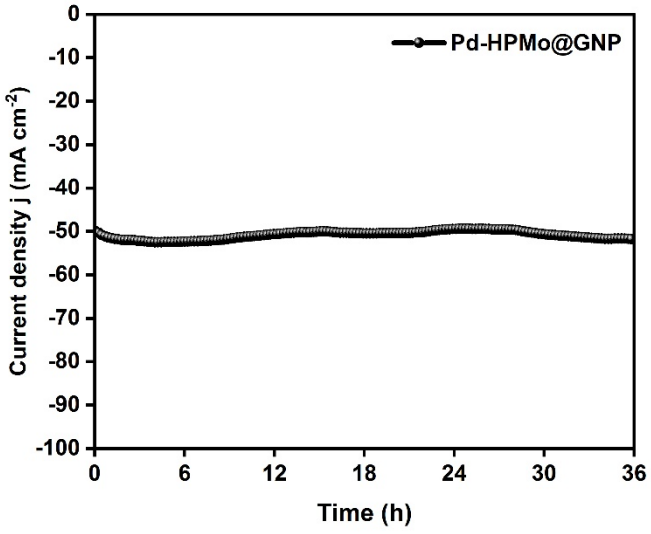

Figure S7. Chronoamperometric analysis of Pd-HPMo@GNP at a -0.25 V (vs. RHE) applied potential for 36 h (Long-term stability test at higher current density).

Characterization analysis of Pd-HPMo@GNP after the long-term stability test

XRD

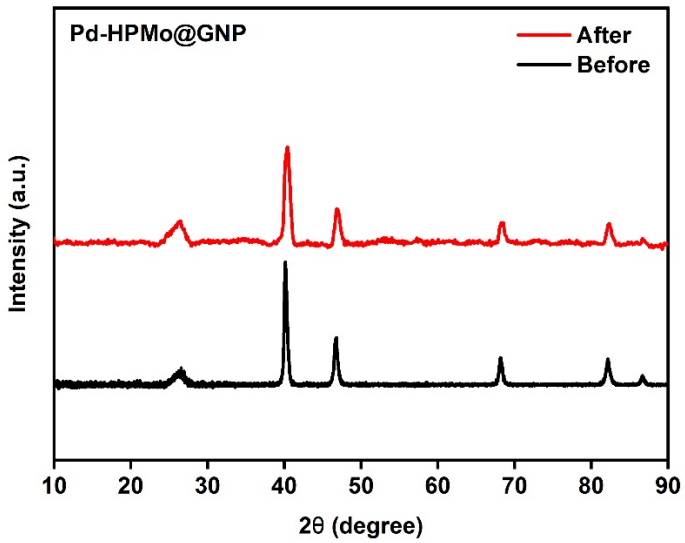

Figure S8. XRD plots of Pd-HPMo@GNP before and after the long-term stability test at higher current density

SEM and HR-TEM

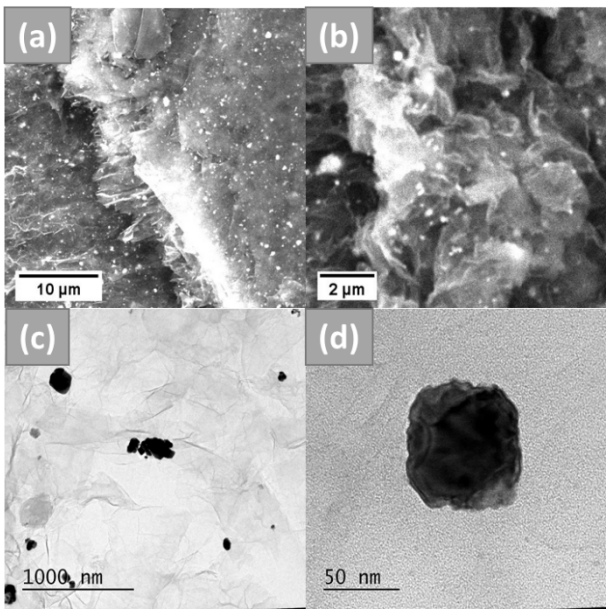

Figure S9. SEM and HR-TEM images of Pd-HPMo@GNP after the long-term stability test.

Table. S1: Comparison of the catalytic performance for 4-nitrophenol reduction

Material	**Concentration of 4-NP (mM)**	**Mass of $NaBH_4$ (mg)**	**Catalyst (mg)**	**Volume of 4-NP (mL)**	**Reactivity Time (mins)**	**Ref**
Pd@HZIF-30-2	36	330	33	20	5	[1]
1T-MoS_2/RGO	71.88	0.91	0.2	1	4	[2]
Fe_3O_4@SN/ HPW@CG–Ag	5	9.83	1	0.7	7	[3]
MXene@AgPd/ PDA	0.1	-	0.06	50	1	[4]
Pd/CNT	1	25	1	4	30	[5]
Nb_4C_3@PdNPs	0.133	3	0.033	0.4	2.75	[6]
Ti_3C_2@PdNPs	5	7.57	1	1	8	[7]
CS/GA RGO/Pd	5	3.78	1	1	64	[8]
RGO@Pd@C	0.1	30	5	3	0.5	[9]
Pd/GO	7.4	15.51	0.25	1	2	[10]
Pd-HPMo	0.43	120	1	50	2	**This work**
Pd-HPMo@GNP	0.43	120	1	50	7	**This work**

Table S2: Evaluation of the electrocatalytic performance of HPMo-derived electrocatalysts for HER.

Catalyst material	Tafel slope ($mV.dec^{-1}$)	Overpotential η_{10} (mV *vs.* RHE)	Electrolyte	Loading mass ($mg.cm^{-2}$)	Ref.
CNT-*g*-PSSCo/PW_{12}	25	31	0.5 M H_2SO_4	-	[11]
Fe-Mo sulfide/carbon composite	62	321	0.5 M H_2SO_4	0.21	[12]
Cu-Mo-P/CC	54.1	145.9	0.5 M H_2SO_4	1.37	[13]
MoP@PC/rGO	53.6	234.6	0.5 M H_2SO_4	0.14	[14]
P-W_2C@NC	53	89	0.5 M H_2SO_4	3.5	[15]
Co/WC@NC	88	158	0.5 M H_2SO_4	0.84	[16]
MoP@PC-CNTs	55.9	220	0.5 M H_2SO_4	-	[17]
CoMoS-600	65.50	235	0.5 M H_2SO_4	-	[18]
PMo/ZIF-67-6-6 N	50	83	0.5 M H_2SO_4	0.708	[19]
MoWOSP@C	74.1	118	0.5 M H_2SO_4	0.34	[20]
Mo_2C@C (S-800)	71	47	0.5 M H_2SO_4	0.45	[21]
MoC_x@C-1	56	79	0.5 M H_2SO_4	0.354	[22]
Pd-HPMo	175	240	0.5 M H_2SO_4	0.1035	**This work**
Pd-HPMo@GNP	90	94	0.5 M H_2SO_4	0.1035	**This work**

Table S3: Elemental composition of Pd-HPMo@GNP based on the ICP-MS analysis

Sample replicates	95 Mo (ppm)	105 Pd (ppm)
Before 1	0.93	15.35
Before 2	1.01	15.31
Mean (before)	**0.97**	**15.33**
After 1	0.37	15.16
After 2	0.39	15.77
Mean (after)	**0.38**	**15.47**

References

1. H. Jiang, M. Liu, M. Zhou, Y. Du and R. Chen, *Industrial & Engineering Chemistry Research*, 2021, **60**, 15045-15055.
2. N. Meng, J. Cheng, Y. Zhou, W. Nie and P. Chen, *Applied Surface Science*, 2016, **396**.
3. Z. Wang, S. Zhai, B. Zhai, Z. Xiao, F. Zhang and Q. An, *New Journal of Chemistry*, 2014, **38**, 3999-4006.
4. J. Jin, S. Wu, J. Wang, Y. Xu, S. Xuan and Q. Fang, *Dalton Trans.*, 2023, **52**, 2335-2344.
5. J. Audevard, A. Benyounes, R. Castro Contreras, H. Abou Oualid, M. Kacimi and P. Serp, *ChemCatChem*, 2022, **14**, e202101783.
6. N. Shabana, A. M. Arjun and P. A. Rasheed, *New J. Chem.*, 2022, **46**, 13622-13628.
7. J. Yin, L. Zhang, T. Jiao, G. Zou, Z. Bai, Y. Chen, Q. Zhang, M. Xia and Q. Peng, *Nanomaterials*, 2019, **9**, 1009.
8. L. Ge, M. Zhang, R. Wang, N. Li, L. Zhang, S. Liu and T. Jiao, *RSC Advances*, 2020, **10**, 15091-15097.
9. Z. Zheye, F. Xiao, J. Xi, T. Sun, S. Xiao, H. Wang, S. Wang and Y. Liu, *Scientific reports*, 2014, **4**, 4053.
10. W. Sun, X. Lu, Y. Tong, Z. Zhang, J. Lei, G. Nie and C. Wang, *International Journal of Hydrogen Energy*, 2014, **39**, 9080–9086.
11. Y. Lin, Y. Zhu, Q. Ma, X. Ke, P. Ma, R. Liao, S. Liu and D. Wu, *Macromol. Rapid Commun.*, 2022, **43**, 2100915.
12. Z. Huang, Z. Yang, M. Z. Hussain, Q. Jia, Y. Zhu and Y. Xia, *J. Mater. Sci. Technol.*, 2021, **84**, 76-85.
13. Y.-J. Tang, Y. Chen, H.-J. Zhu, A. M. Zhang, X.-L. Wang, L.-Z. Dong, S.-L. Li, Q. Xu and Y.-Q. Lan, *J. Mater. Chem. A*, 2018, **6**, 21969-21977.
14. J. i. Li, J. i. Li, X. R. Wang, S. Zhang, J. Q. Sha and G. u. Liu, *ACS Sustain. Chem. Eng.* , 2018, **6**, 10252-10259.
15. G. Yan, C. Wu, H. Tan, X. Feng, L. Yan, H. Zang and Y. Li, *J. Mater. Chem. A*, 2017, **5**, 765-772.
16. D. Sun, Y. Fu, Y. Liu, J. Li, L. Men, B. Sun, A. Geng, X. Li and Z. Su, *J. Solid State Chem.*, 2022, **308**, 122879.
17. J.-S. Li, X.-R. Wang, J.-Y. Li, S. Zhang, J.-Q. Sha, G.-D. Liu and B. Tang, *Carbon*, 2018, **139**, 234-240.

18. Z. Huang, Z. Yang, Q. Jia, N. Wang, Y. Zhu and Y. Xia, *Nanoscale*, 2022, **14**, 4726-4739.
19. C. Chen, A. Wu, H. Yan, Y. Xiao, C. Tian and H. Fu, *Chem. Sci.*, 2018, **9**, 4746-4755.
20. X.-D. Wang, Y.-F. Xu, H.-S. Rao, W.-J. Xu, H.-Y. Chen, W.-X. Zhang, D.-B. Kuang and C.-Y. Su, *Energy Environ. Sci.*, 2016, **9**, 1468-1475.
21. Y. Y. Chen, Y. Zhang, W. J. Jiang, X. Zhang, Z. Dai, L. J. Wan and J. S. Hu, *ACS nano*, 2016, **10**, 8851-8860.
22. X. Yang, X. Feng, H. Tan, H. Zang, X. Wang, Y. Wang, E. Wang and Y. Li, *J. Mater. Chem. A*, 2016, **4**, 3947-3954.